



## Seismic Effects and Static Analysis for the Artificial Damped Outrigger Systems in Tall R.C Buildings

Dr. Abbas A. Allawi

Assistant Professor

College of Engineering - University of Baghdad

E-mail: abbasallawi2004@yahoo.com

Amneh Hamid Al Mukhtar

M. Sc. Student

College of Engineering- University of Baghdad

E-mail: [amena1981eng@gmail.com](mailto:amena1981eng@gmail.com)

### ABSTRACT

This paper studies the combination fluid viscous dampers in the outrigger system to add supplementary damping into the structure, which purpose to remove the dependability of the structure to lower variable intrinsic damping. It works by connecting the central core, comprising either shear walls or braced frames, to the outer perimeter columns.

The modal considered is a 36 storey square high rise reinforced concrete building. By constructing a discrete lumped mass model, and using frequency-based response function, two systems of dampers, parallel and series systems are studied. The maximum lateral load at the top of the building is calculated, and this load will be applied at every floor of the building, giving a conservative solution. For static study **Equivalent Lateral Force (ELF)** was conducted. **MATLAB** software, has been used in this study.

From analysis data, it is observed that the parallel system of dampers result lower amplitude of vibration and achieved more efficiently compared to the series system, and the horizontal displacement for each configurations by using MATLAB software is less than the analytical solution using a uniformly distributed load of 36 nodal point forces that divided the total height.

**Key words:** outrigger system, fluid viscous damper, discrete model.

### التأثيرات الزلزالية والتحليل الاستاتيكي لأنظمة دعامة الإخماد الاصطناعي في المباني الخرسانية المسلحة العالية

أمينة حامد المختار  
طالبة ماجستير  
كلية الهندسة-جامعة بغداد

د. عباس عبد المجيد علاوي  
استاذ مساعد  
كلية الهندسة-جامعة بغداد

### الخلاصة

تتناول هذه الدراسة عملية دمج مخمدات السائل اللزج في نظام الدعامة لإضافة إخماد تكميلي للمنشأ ، والذي يهدف إلى إزالة اعتماد المنشأ على القيمة المنخفضة للإخماد الجوهري. وهي تعمل عن طريق ربط النواة المركزية (the central core) ، التي تضم إما جدران القص أو هيكل مدعوم، إلى الأعمدة الخارجية المحيطة. النموذج الذي تم دراسته هو بناية شاهقة الارتفاع من الخرسانة المسلحة تتكون من 36 طابق وذات مقطع مربع. تتمحور الدراسة من خلال انشاء نموذج من كتل متجمعة منفصلة، واستعمال دالة الاستجابة المعتمدة على التردد، لنظامين من المخمدات، وهما نظاما التوازي والتوالي. تم احتساب الحد الأقصى للحمل الجانبي في الجزء العلوي من المبنى، وطبق هذا الحمل لكل طابق من المبنى، معطيا حلا محافظا. تم استعمال طريقة القوة الجانبية المكافئة للحالة الاستاتيكية. تم استخدام برنامج MATLAB في هذه الدراسة.

لوحظ من تحليل البيانات أن المخمد السائل اللزج بوضعية التوازي ينتج ذبذبات ذات قيم أقل ويحقق كفاءة أكثر مقارنة بوضع المخمد بوضعية التوالي. باستعمال برنامج MATLAB تكون الإزاحات الأفقية لكلا النظامين أقل من طريقة التحليل باستعمال حمل يوزع بشكل منتظم على 36 نقطة عقدية مقسومة على الارتفاع الكلي.

**الكلمات الرئيسية:** نظام الدعامة، مخمد السائل اللزج، نموذج منفصل.

## 1. INTRODUCTION

Outrigger is a common system of strengthening and stiffening tall buildings. It works by connecting the central core, comprising either braced frames or shear walls, to the outer perimeter columns. The explication of building outrigger behavior is easy because outriggers represent as firm arms engaging external columns, at the point when a core have a tries to incline, its rotation at the outrigger level generates a tension- compression couple in the external column moving contrary to that movement. As the outcome, the outrigger restrict the bending of the core by introducing a point of inflection in the deflection profile, as shown in **Fig.1**. Thus decreasing the lateral motion at the top when the reversal in curvature, **Nanduri, et al., 2013; and Melek, et al., 2012**.

Besides at the outrigger intersection lowering the core moment, the system equals the differential shortening of exterior columns coming from axial load imponderables and temperature. Another influence of using outriggers is the considerable lowering of net tension and uplift force at the foundation level, **Choi, et al., 2012**.

The damped outrigger system works by the insertion of viscous dampers between the external columns and the outriggers. When it was done, there was a considerable rise in damping, **Willford, and Simith, 2008**. Therefore, the outrigger system was used as one of the structural system to control the excessive drift during lateral load due to earthquake load.

## 2. STRUCTURAL DESCRIPTION AND MODELING

### 2.1 Structural Parameters

The modal considered in this study is a **36** storey square high rise reinforced concrete building with a base dimension of **30 m** by **30 m**. The floor to floor height is **4 m** contributing to a total building height of **144 m**. The building has a **14 m** by **14 m** central concrete core with a thickness of **45 cm**. The building has two outrigger arms cantilevering from the core to the perimeter columns from each of the side of the core. **W14X398** sections with an approximate cross-section area of **0.15 m<sup>2</sup>** used as the perimeter columns, **Gamaliel, 2008; and Smith, and Willford, 2007**.

The gravity system used in conjunction with central concrete core consists of **25 cm** thick reinforced concrete slabs, with beams section of **45 cm X 70 cm**, and square reinforced concrete columns (**45 cm X 45 cm**). **Fig. 2** summarizes the building dimensions described.

### 2.2 Structural Model

To create a realistic modal of the proposed building described in section **2.1**, each floor of the building will be modeled as a series of masses lumped at the center of the core. Each mass has two degrees of freedom, the vertical translation degree of freedom has been neglected to simplify the modal, as shown in **Fig. 3**.

The general discrete equation of motion written in matrix form as

$$M \ddot{U} + C \dot{U} + K U = P \quad (1)$$

To obtain the global stiffness matrix, the direct stiffness approach is used. A standard two-node member element with two degrees of freedom for each node is considered in this study. The element stiffness matrix are given by



al., 2008. While some studies using the intrinsic damping ratio of 2.5% for 50 storey high rise reinforced concrete building, Melek, et al., 2012.

### 2.3 The Damped Outrigger Concept

The concept of the damped outrigger is shown in Figs. 4,5 and 6. Fig. 4 appears how the outrigger systems activate in easy conditions while incorporated inside a usual core-to-perimeter columns outrigger systems. As a structure subjects dynamic sway motion, there is proportional vertical motion between the ends of stiff outrigger element that cantilevering from the core and the perimeter column. There are needful for the outriggers to shift vertically proportional to the floor at these levels, while the floors bend in double curvature to stay attached to the outer columns and the central core. The dampers are incorporated across this building discontinuity, dissipating energy through the cyclic motion, and producing the raise in the total damping for the structure. Fig. 5 shows in terms of a conceptually the form of detail commonly wanted at the level where the damper is incorporated. The arranging can be as shown in Fig. 6 at the outriggers level in this situation, Smith, and Willford, 2007.

### 2.4 The Damped Outrigger Model

While the concept given by Willford and Smith, 2008 implies that the perimeter columns is in series configuration with the dampers, as well be studied parallel configuration of columns and dampers by Gamaliel, 2008 to provide a good comparative study, as shown in Fig. 7.

The approach to drive typical damper characteristic is based on macroscopic point of view. Where in this point of view, the stiffness is defined based on the slope of the diagonal line of the hysteresis loop and the damping is derived from the hysteresis loop of tested damper, Al Mallah, 2011. Then, obtain the equivalent complex stiffness for both parallel and series configuration.

#### 2.4.1 Hysteresis loop and characteristics of tested damper

Considering a simple single degree of freedom (SDF) system with a viscous damper is subjected to a harmonic load, under steady- state response, the damping force equals to:

$$\begin{aligned} P(t) &= C_o \frac{du}{dt} = C_o \omega u_o \cos(\omega t - \delta) = C_o \omega \sqrt{u_o^2 - u^2} \sin^2(\omega t - \delta) \\ &= C_o \omega \sqrt{u_o^2 - [u(t)]^2} \end{aligned} \quad (7)$$

$$\left(\frac{u}{u_o}\right)^2 + \left(\frac{P(t)}{C_o \omega u_o}\right)^2 = 1 \quad (8)$$

Which is the equation of the ellipse shown in Fig. 8. The area in closed by the ellipse is  $\pi (u_o)(C_o \omega u_o) = \pi C_o \omega u_o^2$ , which is equal to the dissipated energy

$$E_D = 2\pi \zeta \frac{\omega}{\omega_n} K u_o^2 \quad (9)$$

Due to harmonic force with  $\omega = \omega_n$ , and based on macroscopic point of view, the loose stiffness,  $K_2$  is defined based on the slope of the diagonal line of the hysteresis loop. The damping coefficient,  $C_o$ , is equal to the loose stiffness divided by  $\omega$ , and is also calculated from above as:

$$C_o = \frac{E_D}{\pi \omega u_o^2} \quad (10)$$

The equivalent damping ratio  $\zeta_{eq}$  calculated from a test at  $\omega = \omega_n$  would not be right at any exciting frequency, but it would be a satisfying approximation.

$$\zeta_{eq} = \frac{1}{4\pi} \frac{E_D}{E_{SO}} \quad (11)$$

Where the strain energy,  $E_{SO} = K u_o^2 / 2$  is calculated from the stiffness  $K$  resolved by experience, **Chopra, 2008**. Based on the above,  $C_o$  and  $\zeta_{eq}$  can be calculated from hysteresis loop of the tested dampers.

The model considered for this study is based on that the material behavior is in linear elastic range. However, it must be mentioned that most dampers classified as viscous dampers do not behave fully linear over the range of the entire velocity due to nonlinear material behavior and sealing friction which ends up in a nonlinear viscous behavior at small velocities.

#### 2.4.2 Derivation of equivalent complex stiffness

Damping introduces complexity to the solution by adding a term involving velocity. In order to define the complex frequency-response function, the steady-state motion of a **SDOF** system is applied for both parallel and series configuration, which the equivalent complex stiffness can be expressed as:

- Parallel configuration, The harmonic motion at the forcing frequency,  $\omega$ , can be expressed as

$$u(t) = H_u(\omega) e^{i\omega t} \quad (12)$$

$$\dot{u}(t) = i\omega H_u(\omega) e^{i\omega t} \quad (13)$$

The equation of motion for the parallel configuration of damper and column is

$$p(t) = k_{col} u(t) + C \dot{u}(t) = (k_{col} + i\omega C) H_u(\omega) = k_{eq} H_u(\omega) \quad (14)$$

$$\therefore k_{eq} = k_{col} + i\omega C \quad (15)$$

, **Chopra, 2008** and **Gamaliel, 2008**, See **Fig. 9**.

-Series configuration, The harmonic motion at the forcing frequency,  $\omega$ , can be expressed as

$$u(t) = H_u(\omega) e^{i\omega t}, \text{ and } u(t)_1 = H_{u1}(\omega) e^{i\omega t} \quad (16)$$

$$\dot{u}(t) = H_u(\omega) e^{i\omega t}, \text{ and } \dot{u}(t)_1 = i\omega H_{u1}(\omega) e^{i\omega t} \quad (17)$$

Then, the equation for the series configuration of damper and column is:

$$p(t) = k_{col} u(t)_1 = C (\dot{u}(t) - \dot{u}(t)_1) \quad (18)$$

$$(i\omega C) H_u(\omega) = (k_{col} + i\omega C) H_{u1}(\omega) \quad (19)$$

$$H_{u1}(\omega) = \frac{i\omega C}{k_{col} + i\omega C} H_u(\omega) \quad (20)$$

$$p(t) = \frac{k_{col} i\omega C}{k_{col} + i\omega C} H_u(\omega) = k_{eq} H_u(\omega) \quad (21)$$

$$\therefore k_{eq} = \frac{k_{col} i\omega C}{k_{col} + i\omega C} \quad (22)$$

,Chopra, 2008 and Gamaliel, 2008, See Fig. 10. The above procedure has been derived the equivalent complex stiffness for both parallel and series damper configuration. The next step is to obtain the rotational stiffness at the outrigger level.

### 2.4.3 Derivation of the rotational stiffness

The column-restrained outriggers oppose the rotation of the core, when subjected to lateral loads, causing the moments and the lateral deflections in the core to be minimal than if the freestanding core alone resisted the loading. The exterior moment is now resisted not by bending of the core alone, but also by the axial compression and tension of the exterior column connected to the outrigger, Taranath, 2010.

The axial shortening and elongation of column is clearly equal to the rotation of the core multiplied by their particular distances from the exterior column to the center of the core. If the distance of the equivalent columns is  $d/2$  from the central core, the axial distortion of the columns is then equal to  $\beta d/2$ , where  $\beta$  is the core rotation. Then the stiffness of the equivalent spring is studied for unit rotation of the core (i.e.,  $\beta = 1$ ), therefore the axial deformation of the equivalent columns is equalize to  $1 \times d/2 = d/2$  units, Taranath, 2010.

The corresponding axial load is as following

$$p(t) = A E d/2 (aH) \quad (23)$$

$p(t)$  is the column axial load;  $A$  is the column area;  $E$  is the modulus of elasticity;  $d$  is the distance from the center of core to the exterior column;  $aH$  is the height at the outrigger level. Using the notion  $K_R$  for the rotational stiffness, and noticing that there are two equivalent columns, each situated at a distance from the core, we obtain

$$K_R = p(t) \times d/2 \times 2 \quad (24)$$

$$K_R = \frac{A E d^2}{2 aH} \quad (25)$$

The addition of rotational stiffness to the core at the outrigger level can be obtained as follows

$$M = p(t) \times d/2 \quad (26)$$

Where,  $p(t) = k_{eq} H_u(\omega)$ ,  $H_u(\omega) = \frac{d}{2} \beta$ , and  $M = K_R \beta$

$$\therefore K_R = k_{eq} \left(\frac{d}{2}\right)^2 \quad (27)$$

## 2.5 Applying Outrigger Effect to Discrete Model

The effect of the outrigger can be modeled by introducing a minor change in the stiffness matrix. A rotational spring is to be added to the nodal point where the outrigger is located. Hence, the outrigger nodal point will have a modified rotational stiffness comprised of the existing rotational stiffness from the core (cantilever beam) and the rotational stiffness,  $K_R$ , from the outrigger. From previous section, the value of  $K_R$  has been derived. Because the Damping introduces complexity to the solution by adding a term involving velocity, the equivalent complex stiffness has been derived for both parallel and series damper configuration, and has been incorporated this effect into the stiffness matrix of the core, **Gamaliel, 2008 and Taranath, 2010**.

In the case of a damped outrigger, the damping matrix,  $C$ , is required to solve the full differential equation of motion. The conventional approach is to work in the real domain by constructing the damping matrix and introducing the damping coefficient  $C_o$  at the location corresponding to the rotation of the outrigger node. However, it is algebraically more convenient to work in the complex domain, by collapsing the  $C$  matrix altogether and lumping the effect of damping into the stiffness matrix, forming an equivalent complex stiffness matrix, **Gamaliel, 2008**, which has been obtained in section 2.4.1.

## 3. STATIC ANALYSIS

### 3.1 Equivalent Lateral Force (ELF) Analysis

The ground motion risks that rely on the regional seismicity depending upon a list of basics. Then considered to be ingrained in building designed to **ASCE 7-05** the design ground motions are depend on the margin of a minimal bound evaluation versus collapse. Depend on experiment this minimal bound has been believed in ground motion to be almost a factor of **1.5**, **Taranath, 2005**. Subsequently, the design earthquake ground motion has been selected at a ground motion shaking level that is **1/1.5**, which is equal to the **2/3** of the **MCE** ground motion.

**ASCE 7-05** explains the **MCE** ground motion at short periods,  $S_s$ , in terms of the mapped values of the spectral response acceleration and also at 1 second,  $S_1$ , for site class  $B$  for soft rock. These values may be gained from the map developed by **USGS**. The maps developed by **USGS** define sites of fault using both the probabilistic and deterministic proceedings, and contours of random horizontal acceleration values, **Taranath, 2005**.

In this study, the parameters  $S_s$  and  $S_1$  determine from the major map developed by **USGS**, in Irvine, California for site class  $D$ , using an importance factor,  $I_E$ , is equal to **1** for the Occupancy Category **II**, and the effective seismic weight,  $W_x$  at each node is equal to **12,000 KN**.

The seismic base shear,  $V$ , in accordance with (**Eq. 12.8-1, ASCE 7-05**) is

$$V = C_s W t \quad (28)$$

The seismic response coefficient,  $C_s$ , shall be determined in accordance with the following equation:

$$C_s = \frac{SDS}{\left(\frac{R}{I_E}\right)} \quad (29)$$

Where,  $SDS$ , design spectral response accelerations;  $R$ , response modification factor see (**Table 12.2-1, ASCE 7-05**).

Observing **ASCE 7-05** does not give a separate formula for calculating the concentrated force  $Ft$  at top. Its effect is automatically included in the manner in which the base shear,  $V$ , is



distributed vertically over the building height. For a structure with  $n$  levels, the force at diaphragm level  $x$  is given by the equation:

$$F_x = C_{vx} V \tag{30}$$

Where,  $C_{vx}$  = vertical distribution factor.

### 3.2 Static Analysis of Single Outrigger

#### 3.2.1 Optimum location of the single outrigger

The preceding analysis has assigned to that the useful action of outrigger is a function of two special characteristics: (1) the stiffness of the equivalent spring; and (2) the value of the rotation at the spring location of the cantilever due to lateral loads. The spring stiffness, which is derivation in **Section 2.4.3**, is a function of column length beneath the outrigger site, which differs inversely as the distance of the outrigger from the base. For example, the stiffness is at a minimal when the outrigger exists at the top and a maximum when at the bed.

On the other hand, the rotation,  $\theta_w$ , of the free cantilever subjected to a uniformly lateral load differs parabolically at the top with a maximum value to zero at the bottom. Therefore, from the point of view of spring stiffness, it is eligible to set the outrigger at the bottom, whereas from estimation of its rotation, the converse is true. It must therefore be clear that the optimum location is somewhere in between.

To evaluate the optimum location, first the restoring moment,  $M_x$ , of the outrigger situated at  $x$  is estimated. Next, a equation for the deflection at the top of the core due to  $M_x$  is derived. Differentiating this equation and equating a zero results in a third-degree polynomial, the solution of which yields the outrigger optimum location identical to the minimum deflection at top of the building due to external load. The rotation  $\theta_w$  of the cantilever at a distance  $x$  from the top, due to uniformly distributed load  $w$ , is the derivative of its deflection profile, is given by the relation:

$$\theta_w = \frac{w}{6EI} (X^3 - L^3) \tag{31}$$

The rotation due to the restoring couple  $M_x$  is given by the relation:

$$\theta_x = \int_0^{L-X} \frac{Mx}{EI} dx = \frac{Mx}{EI} (L - X) \tag{32}$$

Knowing the rotational stiffness  $K_R$ , one can find the moment in the spring  $M_x$ , by satisfactory the rotation compatibility relation at a distance  $x$  from the top. The final rotation of the cantilever

$$\frac{w}{EI6} (-L^3 + X^3) - \frac{Mx}{EI} (-X + L) = \frac{Mx}{K_R} \tag{33}$$

The negative sign mentions that the rotation of the cantilever due to external load acts in a direction opposite to the rotation due to the spring stiffness.

$$\frac{w}{EI6} (-L^3 + X^3) = Mx \left[ \frac{(-X+L) \times 2}{A E_{col} d^2} + \frac{(-X+L)}{EI} \right]; \text{ Let } g = \frac{1}{A E_{col} d^2} + \frac{1}{2EI}$$

$$Mx = \frac{w(X^3-L^3)}{12EI(L-X)g} \tag{34}$$



Next, the deflection at the top due to  $Mx$  is obtained, by the integration of the Bending-Moment Equation:

$$u(L)_x = \frac{Mx}{2EI} (L - X)(L + X) \tag{35}$$

The optimum location of the outrigger is that location for which the deflection  $u(L)_x$  is a maximum. This is gained by substituting  $Mx$  into the equation above and differentiating with respect to a distance  $x$  from the top and equating to zero.

$$u(L)_x = \frac{w(X^3 - L^3)(L - X)(L + X)}{24EI^2(L - X)g} = \frac{w(-L^3 + X^3)(L + X)}{EI^2 24g} \tag{36}$$

Thus,  $dy/dx$  of,  $0 = \frac{w(3X^2L + 4X^3 - L^3)}{24EI^2g}$

This cubic equation has a single positive root,  $x = 0.445L$ . Therefore, to minimize drift, the outrigger must exist at a distance  $x = 0.455L$  from the top or, say, approximately at midheight of the building. This corresponds most closely to story number 19.

### 3.2.2 Deflection calculations

The two major limitation of an outrigger systems are the maximum moment at the base of the building, and also the horizontal deflection at the top of the building. The maximum horizontal deflection needs to be below an acceptable limit of human comfort. The moment at the base has no effect on human comfort, but has a great effect in the overall building cost as far as member sizes and foundation system, **Gamaliel, 2008**.

A simple cantilever beam subjected to uniform loading is considered and the deflection profile is given by:

$$u(x) = \frac{W}{24 EI} (X^4 - 4XL^3 + 3L^4) \tag{37}$$

where the value,  $X$ , is the distance from the top. Then the deflection at the top due to uniform load is

$$u(L)_1 = \frac{W L^4}{8 EI} \tag{38}$$

The deflection at the top due to  $Mx$ , which  $Mx$  under the outriggers restraint is the resorting moment, is

$$u(L)_2 = \frac{Mx}{2EI} (L - X)(L + X) \tag{39}$$

The deflection at the top is simply the superposition of the cantilever beam due to the moment induced by the rotational spring and due to the uniform load:

$$u(L)_{1,2} = \frac{W L^4}{8 EI} - \left[ \frac{Mx}{2EI} (L - X)(L + X) \right]$$

$$u(L)_{1,2} = \frac{W L^4}{8 EI} - \frac{w(-L^3 + X^3)(L + X)}{24EI^2g}, \text{ Let } f = 3 EI \times g = \frac{3 EI}{A E_{cot} d^2} + \frac{3}{2}$$



$$u(L)_{1,2} = \frac{w L^4}{8EI} - \frac{w(X^4 + X^3L - XL^3 - L^4)}{8EI^2 f}$$

$$u(L)_{1,2} = \frac{w}{8EI} \left[ L^4 - \frac{1}{f} (X^4 + X^3L - XL^3 - L^4) \right] \quad (40)$$

The analytical solution, by using a uniformly distributed load of **36** nodal point forces that divided the total height, gives a value of **0.224 m**.

### 3.3 Static Analysis Using Software Program

The different outrigger systems appoint the use of viscous dampers. The discrete model is run in MATLAB software for four different configurations,

- (1) outrigger with damper in series;
- (2) outrigger with damper in parallel;
- (3) outrigger without damper;
- (4) system without outrigger.

For static case, the forcing frequency  $\omega$  is set to zero for each series and parallel configurations. Therefore, mathematically it can be shown as  $\omega \rightarrow 0$ ; the equivalent stiffness for series is:

$$k_{eq} = \frac{k_{col} i\omega C}{k_{col} + i\omega C} \rightarrow 0 \quad (41)$$

This proposes that the outrigger system with series damping behaves completely as a system without outrigger under static loading. For parallel the equivalent stiffness is

$$k_{eq} = (k_{col} + i\omega C) \rightarrow k_{col} \quad (42)$$

This implies that the outrigger with parallel damping configuration behaves as a typical outrigger under static load.

The matrix equation run in MATLAB to be solved is:

$$k_{eq} U = P \quad (43)$$

The outrigger location must be the addition of the rotational stiffness to the core for each configuration. **Fig. 11** shows the horizontal displacement along the height of the building for each configurations. It can be seen that the curve for configuration (1) and configuration (4) matched with each other, and the curve for configuration (2) matched with the curve for configuration (3). The horizontal displacement for configuration (1) and configuration (4) at the top of the building is equal to **0.206 m**, and for configuration (2) and configuration (3) at the top is equal to **0.1976 m**.

### 3.4 Story – Drift Limit

The story drift,  $\Delta_x$ , is calculated from previous analysis, from data of **Fig. 11**, compared with the allowable story drift ( $\Delta_a$ ) as gained from (**ASCE 7-05, Table 12.12-1**), for any story.

The allowable drift ( $\Delta_a$ ) in the **ASCE 7-05** is based on the selected building system and dependent on building occupancy category. From **ASCE 7-05, Table 12.12-1**, the value of ( $\Delta_a$ ) is equal for any story (**0.08 m**), because the story height is equal for any story.

The determination of story drift,  $\Delta_x$ , uses the next steps:

1. Determine the horizontal displacement at each floor levels by an elastic analysis of the building under the design base shear(see **Fig. 11**). The horizontal displacement at floor level  $x$ , obtained from this analysis, is termed  $\delta x_e$ . The subscript “ $e$ ” stands for elastic analysis.
2. Increase  $\delta x_e$  by the deflection amplification factor,  $Cd$  ; see (Table **12.2-1, ASCE 7-05**), for  $Cd$  values. The resulting quantity,  $Cd \delta x_e$ , is an estimated design earthquake displacement at floor level  $x$ . **ASCE 7-05** requires this quantity to be divided by the importance factor,  $I_E$ , because the forces under which the  $\delta x_e$  displacement is computed are already amplified by  $I_E$ . The quantity  $Cd\delta x_e/I_E$  at floor level  $x$  is  $\delta x$ , the adjusted design earthquake displacement.

$$\delta x = Cd \delta x_e / I_E \quad (44)$$

3. Calculate the story drift  $\Delta x$  for story  $x$  (the story below floor level  $x$ ) by deducting the adjusted earthquake displacement at the bottom of story  $x$  (floor level  $x - 1$ ) from the adjusted earthquake displacement at the top of story  $x$ :

$$\Delta x = -(\delta x_{x-1}) + \delta x_x \quad (45)$$

The  $\Delta x$  values must be kept within limits, see (**Table 12.12-1, ASCE 7-05**). Two items are noting:

1. The redundancy coefficient,  $\rho$ , is equal to 1.0 for the computation of the design story drift, where a redundancy factor,  $\rho$ , shall be assigned to the seismic force-resisting system in each of two orthogonal directions(**ASCE 7-05**).
2. For determining compliance with the story drift limitations, the deflections,  $\delta x$ , may be calculated corresponding to the fundamental period of the structure(**ASCE 7-05**). The values for  $\Delta x$  and  $\Delta a$  are shown in **Table 1**.

### 3.5 P – Delta Effects

The  $P\Delta$  effects in a given story are due to the eccentricity of the gravity load above that story. If the story drift due to the lateral forces were  $\Delta x$ , the bending moments in the story would be augmented by an amount equal to  $\Delta x$  times the gravity load above the story. The ratio of the  $P\Delta$  moment to the lateral-force story moment is designated as a stability coefficient,  $\phi$ . If the stability coefficient  $\phi$  is less than 0.10 for every story, the  $P\Delta$  effects on story shears and moments and member forces may be neglected. If, however, the stability coefficient  $\phi$  exceeds **0.10** for any story, the  $P\Delta$  effects on story drifts, member forces, shears, etc., must be determined by a rational analysis.

where the stability coefficient ( $\phi$ ) as determined by the following equation(**ASCE 7-05**):

$$\phi = \frac{P_X \Delta x}{V_X h_{SX} Cd} \quad (46)$$

Where,  $P_X$  = the total vertical design load at and above Level  $x$  (**kip** or **KN**), where computing  $P_X$  no individual load factor need exceed **1.0**;  $\Delta x$  = the design story drift as defined in **Sec. 3.4** revolving simultaneously with  $V_X$  (**in** or **mm**);  $V_X$ = the seismic shear force acting between Levels  $x$  and  $x - 1$  (**kip** or **KN**) as determined by the following equation(**ASCE 7-05**):

$$V_X = \sum_{i=x}^n F_i \quad (47)$$



where  $F_i$  = the portion of the seismic base shear ( $V$ ) ( $kip$  or  $KN$ ) induced at Level  $i$ ;  $h_{sx}$  = the story height below Level  $x$  (in. or mm);  $Cd$  = the deflection amplification factor in (Table 12.2-1, ASCE 7-05).

The stability coefficient ( $\phi$ ) shall not exceed  $\phi_{MAX}$  determined as follows (ASCE 7-05):

$$\phi_{MAX} = \frac{0.5}{\beta Cd} \leq 0.25 \quad (48)$$

where  $\beta$  is the ratio of shear demand to shear capacity for the story between Levels  $x$  and  $x-1$ . This ratio is permitted to be conservatively taken as 1.0 (ASCE 7-05). Consequently, the value  $\phi_{MAX}$  is equal to 0.1. The values for  $\phi$  are shown in Table 2.

#### 4. CONCLUSIONS

1. The optimum location of the outrigger is that location at a distance  $x = 0.455L$  from the top or, say, approximately at midheight of the building.
2. The analytical solution, by using a uniformly distributed load of 36 nodal point forces divided the total height, gives a value of 0.224 m.
3. The related results, at the discrete model run in MATLAB software for four different configurations, are as follows:
  - The horizontal displacement for configuration (1) and configuration (4) at the top of the building is equal to 0.2060, and for configuration (2) and configuration (3) at the top is equal to 0.1976. This implies that the outrigger with series damping configuration behaves as a system without outrigger under static loading, and that the outrigger with parallel damping configuration behaves as a regular outrigger under static loading.
  - The horizontal displacement for each configurations by using MATLAB software is less than the analytical solution, 0.224 m.
4. The related results, compared the story drift,  $\Delta_x$ , calculated from previous analysis with the allowable story drift ( $\Delta_a = 0.08$  m) as obtained from (ASCE 7-05) for any story, are as follow:
  - From configuration (1) to configuration (4) the story drift is less than the allowable story drift, which is able to pass the requirement.
5. The stability coefficient  $\phi$  for every story is less than 0.10; therefore, the  $P\Delta$  effect on moments and member forces and story shears may be neglected.
6. From analysis data, the parallel placement of viscous damper result in lower amplitude of vibration compared to when the damper is in series.
7. The result of analysis suggests that viscous dampers should be installed in parallel with the perimeter column where the outrigger connects. However, to achieve this type of parallel connection takes more of a construction challenge than connecting it in line with column as proposed by **Smith and Willford, 2007**. Two columns side by side will be required to connect the damper in parallel.

#### REFERENCES

- Al Mallah, N. M., 2011, *The Use of Bracing Dampers in Steel Building Under Seismic Loading*, Ms. D. Thesis : College of Engineering, University of Baghdad.
- ASCE, 2006, *ASCE Standard 7-05: Minimum Design Loads for Buildings and Other Structures*, American Society of Civil Engineers.



- Choi, H., Ho, G., Joseph, L., Mathias, N., 2012, *Outrigger Design for High Rise Buildings*, Chicago, USA : CTBUH Technical Guides.
- Chopra, A., 2008, *Dynamics of Structures: Theory and Applications to Earthquake Engineering*, New Delhi : Prentice-Hall of India.
- Gamaliel, R., 2008, *Frequency- Based Response Of Damped Outrigger System for Tall Buildings*, Civil and Environmental Engineering, University of California.
- Melek, M., Darama, H., Gogus, A., and Kang, T., 2012, *Effects of Modeling of RC Flat Slabs on Nonlinear Response of High Rise Building Systems*, 15 WCEE.
- Nanduri, R., Suresh, B., and Hussain, I., 2013, *Optimum Position of Outrigger System for High- Rise Reinforced Concrete Buildings Under Wind and Earthquake Loadings*, American Journal of Engineering Research, Vol. 2, pp. 76- 89.
- Sathyanarayanan, K., Vijay, A., and Balachandar, S., 2012, *Feasibility Studies on the Use of Outrigger System for RC Core Frames*, India : Department of Civil Engineering, SRM University.
- Smith, R. J., and Willford, M. R., 2007, *The Damped Outrigger Concept for Tall Building*, Arup, London, UK : John Wiley & Sons, Inc.
- Taranath, B., 2010, *Reinforced Concrete Design of Tall Buildings*, US : Taylor and Francis Group.
- Taranath, B. S., 2005, *Wind and Earthquake Resistant Buildings: Structural Analysis and Design*, California : Marcel Dekken.
- Willford, M., and Simith, R., 2008, *Performance Based Seismic and Wind Engineering For 60 Story Twin Towers in Manila*, Beijing, China : The 14th World Conference on Earthquake Engineering.
- Willford, M., Whittaker, A., and Klemencic, R., 2008, *Recommendations for the Seismic Design of High- Rise Buildings*, Chicago : Council on Tall Buildings and Urban Habitat.

## NOMENCLATURE

$A$  = area of the lumped mass,  $m^2$ .

$aH$  = Height at the outrigger level, m.

$b$  = core length, m.

$C_0$  = damping coefficient, N.s/m,

$Cd$  = deflection amplification factor, dimensionless.

$Cs$  = seismic response coefficient, dimensionless.

$Cvx$  = vertical distribution factor, dimensionless.

$E$  = elastic modulus of the core, Pa.

$E_D$  = energy dissipation, N.m.

$E_{SO}$  = strain energy, N.m.



$F_x$  = the force at diaphragm level  $x$ , kN.  
 $H_u(\omega)$  = Complex frequency-response function, dimensionless.  
 $I$  = moment of inertia of the lumped mass,  $m^4$ .  
 $J$  = nodal rotational inertia,  $Kg\ m^2$ .  
 $K$  = Stiffness matrix, N/m.  
 $K_2$  = loss stiffness, N/m.  
 $K_R$  = Rotational stiffness, N/m.  
 $k_{col}$  = Stiffness of column, N/m.  
 $k_{eq}$  = Equivalent complex stiffness, N/m.  
 $L$  = floor height, m.  
 $M$  = Mass matrix, Kg.  
 $Mx$  = restoring moment, kN.m.  
 $P_t$  = A complex periodic loading function, kN.  
 $S_1$  = Mapped MCE, 5 percent damped, spectral response acceleration parameter at a period of 1, %g.  
 $S_s$  = Mapped MCE, 5 percent damped, spectral response acceleration parameter at short periods, %g.  
 $t$  = core thickness, m.  
 $u$  = displacement of the system and the damper, m.  
 $\dot{u}$  = velocity of the piston, m/s.  
 $u_o$  = amplitude of the displacement, m.  
 $V$  = base shears, kN.  
 $W_i$  = the portion of the total gravity load of the structure at level  $i$ , kN.  
 $W_m$  = effective modal gravity load, kN.  
 $W_x$  = effective seismic weight at each node, kN.  
 $\omega$  = frequency of motion, rad/s.  
 $\omega_n$  = Vibration Natural Frequency, rad/s.  
 $\delta$  = phase angle, rad.  
 $\zeta$  = damping ratio, dimensionless.  
 $\zeta_{eq}$  = equivalent damping ratio, dimensionless.  
 $\beta$  = rotation of the core, rad.  
 $\theta_w$  = rotation of the cantilever at a distance  $x$  from the top, rad.  
 $\varphi$  = stability coefficient, dimensionless.

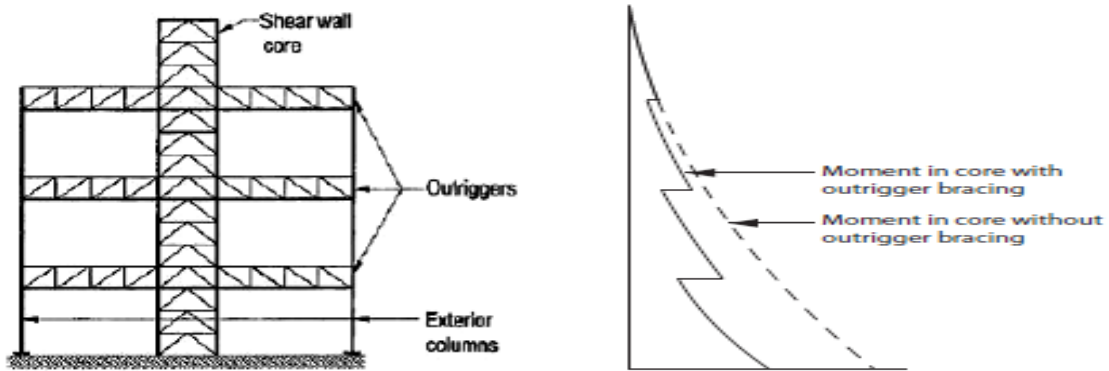


Figure 1. Core – Supported outrigger structures, Sathyanarayanan, et al., 2012.

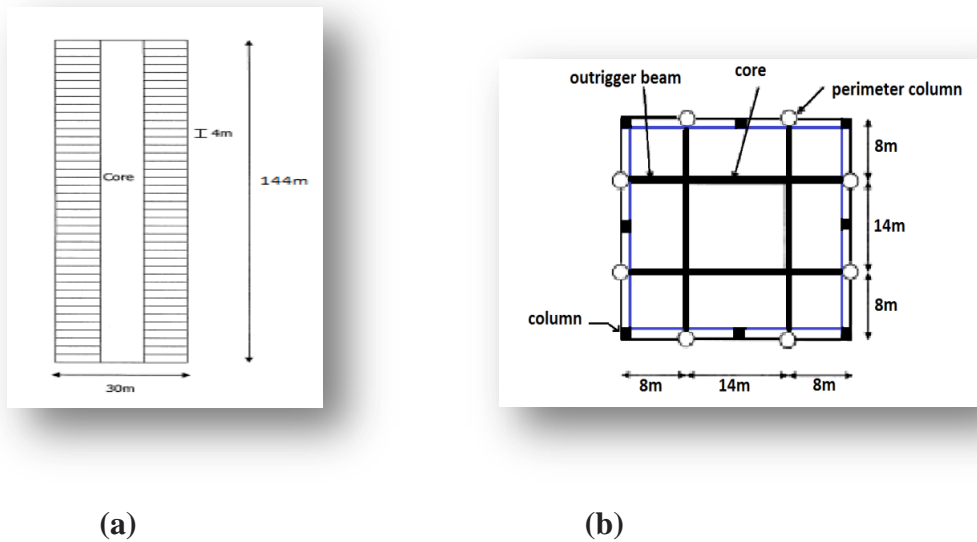


Figure 2. Buildings dimensions (a) in elevation, (b) in plan (some details and beams for gravity system omitted for clarity).

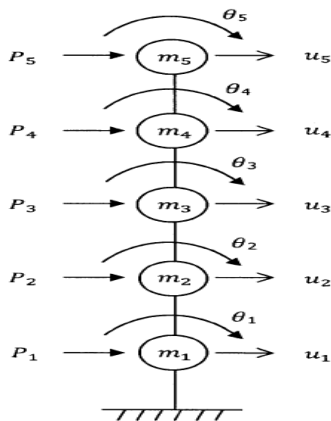
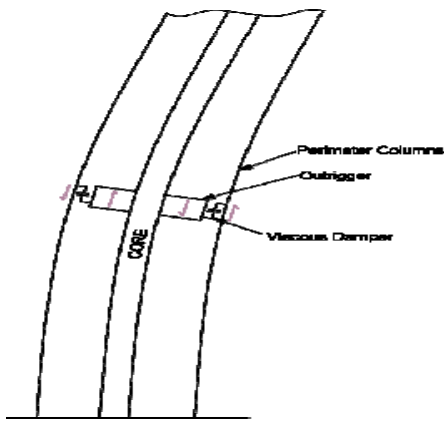
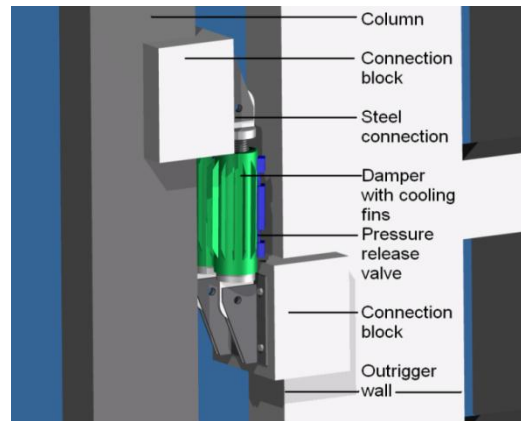


Figure 3. Discrete lumped mass modal for a 5 story building.



**Figure 4.** Patent pending (damped outrigger), Smith, and Willford, 2007.



**Figure 5.** Conceptual detail at outrigger level, Smith, and Willford, 2007.

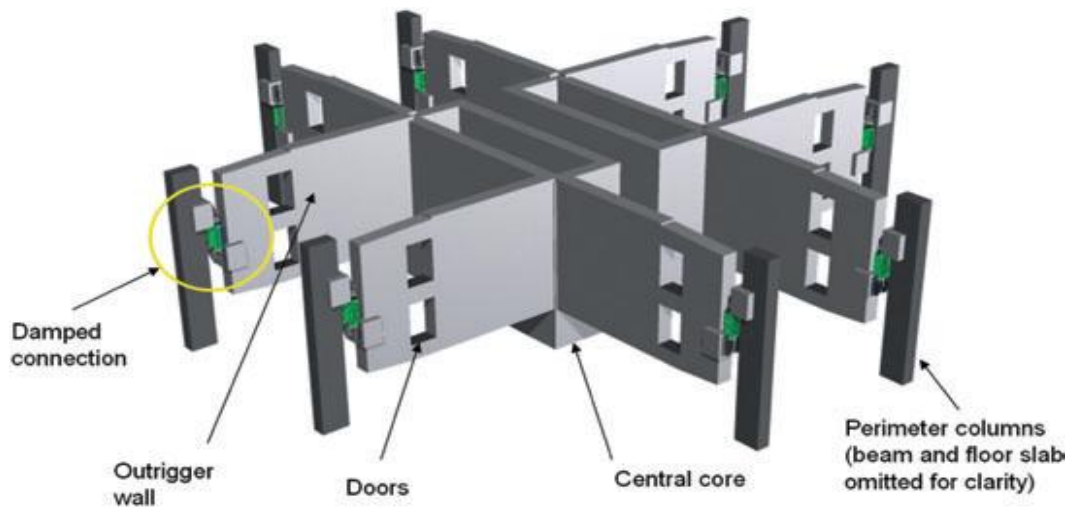


**Figure 6.** General arrangement of outrigger levels, Smith, and Willford, 2007.

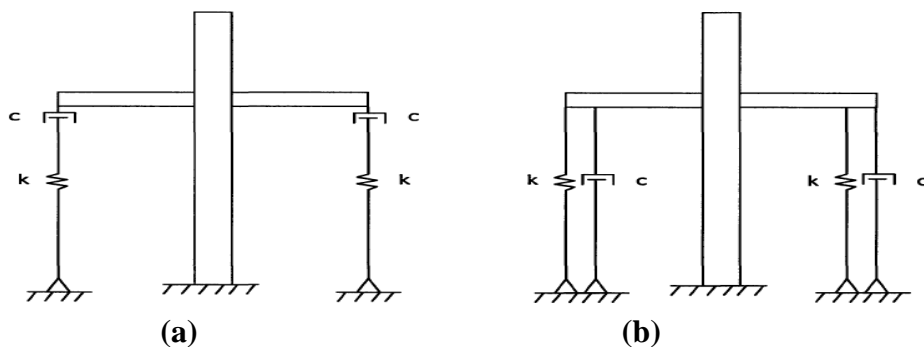


**Figure 7.** Simplified models of the damped outrigger systems in (a) series (b) parallel, Gamaliel, 2008.

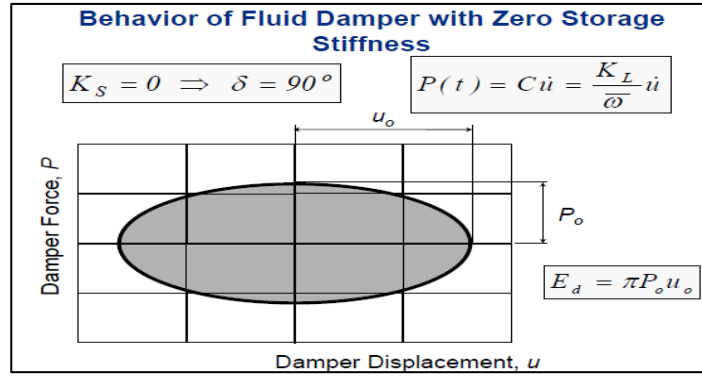


Figure 8. Hysteretic Loop for Viscous Damper

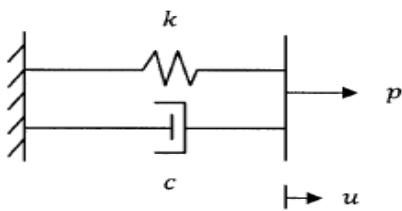


Figure 9. Damper in parallel

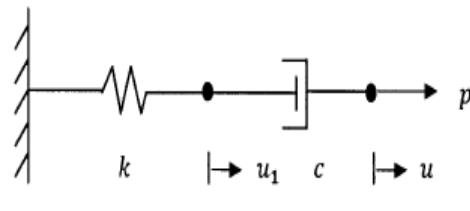


Figure 10. Damper in series

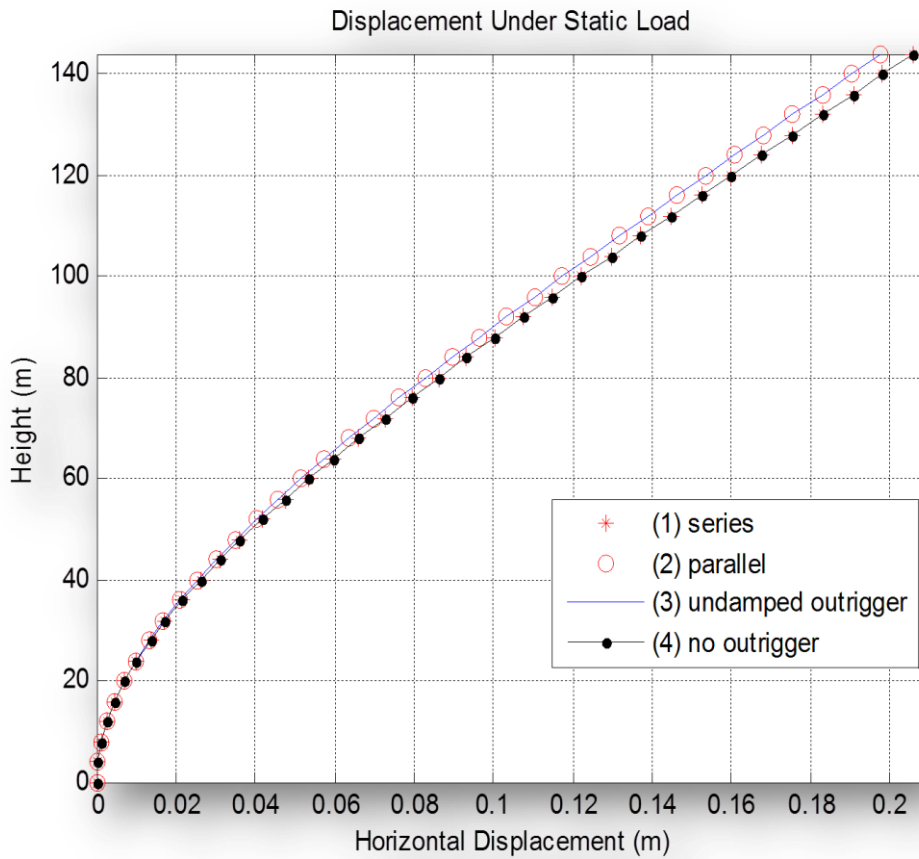


Figure 11. Plot of horizontal displacement profile under static loading.

**Table 1.** (The values for  $\Delta_x$  and  $\Delta_a$ )

<b>Level (from the top)</b>	<b><math>\Delta_x</math>(m) Configuration (1)&amp;(4)</b>	<b><math>\Delta_x</math>(m) Configuration (2)&amp;(3)</b>	<b><math>\Delta_a</math>(m) The allowable drift</b>
36	0.0422	0.0404	0.0800
35	0.0421	0.0404	0.0800
34	0.0420	0.0404	0.0800
33	0.0415	0.0404	0.0800
32	0.0420	0.0403	0.0800
31	0.0420	0.0402	0.0800
30	0.0419	0.0401	0.0800
29	0.0417	0.0400	0.0800
28	0.0415	0.0398	0.0800
27	0.0413	0.0396	0.0800
26	0.0410	0.0392	0.0800
25	0.0406	0.0390	0.0800
24	0.0403	0.0385	0.0800
23	0.0398	0.0380	0.0800
22	0.0392	0.0375	0.0800
21	0.0386	0.0369	0.0800
20	0.0379	0.0361	0.0800
19	0.0371	0.0354	0.0800
18	0.0362	0.0346	0.0800
17	0.0352	0.0338	0.0800
16	0.0342	0.0327	0.0800
15	0.0329	0.0316	0.0800
14	0.0316	0.0303	0.0800
13	0.0302	0.0291	0.0800
12	0.0286	0.0275	0.0800
11	0.0269	0.0260	0.0800
10	0.0251	0.0242	0.0800
09	0.0231	0.0223	0.0800
08	0.0210	0.0204	0.0800
07	0.0188	0.0181	0.0800
06	0.0163	0.0158	0.0800
05	0.0137	0.0134	0.0800
04	0.0110	0.0107	0.0800
03	0.0081	0.0078	0.0800
02	0.0050	0.0048	0.0800
01	0.0017	0.0017	0.0800

Table 2. (The values for  $\varphi$ )

Level (from the top)	$F_i$ (KN)	$V_x$ (KN)	$P_x$ (KN)	$\varphi$ Configuration (1)&(4)	$\varphi$ Configuration (2)&(3)
36	1168	1168	12000	0.0197	0.0189
35	1111	2280	24000	0.0201	0.0193
34	1055	3335	36000	0.0206	0.0198
33	1001	4335	48000	0.0209	0.0203
32	948	5283	60000	0.0217	0.0208
31	896	6180	72000	0.0222	0.0214
30	846	7024	84000	0.0228	0.0218
29	796	7820	96000	0.0233	0.0223
28	748	8568	108000	0.0238	0.0228
27	701	9270	120000	0.0243	0.0233
26	656	9925	132000	0.0248	0.0237
25	612	10537	144000	0.0252	0.0242
24	569	11106	156000	0.0275	0.0246
23	528	11634	168000	0.0261	0.0249
22	488	12122	180000	0.0265	0.0253
21	449	12570	192000	0.0268	0.0256
20	412	12981	204000	0.0271	0.0258
19	376	13357	216000	0.0273	0.0260
18	342	13700	228000	0.0274	0.0262
17	309	14008	240000	0.0274	0.0263
16	277	14284	252000	0.0274	0.0262
15	247	14532	264000	0.0272	0.0261
14	219	14741	276000	0.0269	0.0258
13	192	14933	288000	0.0265	0.0255
12	166	15100	300000	0.0258	0.0248
11	142	15243	312000	0.0250	0.0240
10	120	15363	324000	0.0241	0.0232
09	100	15463	336000	0.0228	0.0220
08	81	15545	348000	0.0214	0.0208
07	64	15670	360000	0.0196	0.0189
06	48	15694	372000	0.0176	0.0170
05	35	15715	384000	0.0152	0.0149
04	23	15738	396000	0.0126	0.0122
03	14	15752	408000	0.0095	0.0092
02	6	15759	420000	0.0061	0.0058
01	2	15761	432000	0.0021	0.0021